

2006

Intensity-modulated radiation therapy dose maps: the matchline effect

Puangpen Tangboonduangjit
University of Wollongong

Follow this and additional works at: <https://ro.uow.edu.au/theses>

University of Wollongong

Copyright Warning

You may print or download ONE copy of this document for the purpose of your own research or study. The University does not authorise you to copy, communicate or otherwise make available electronically to any other person any copyright material contained on this site.

You are reminded of the following: This work is copyright. Apart from any use permitted under the Copyright Act 1968, no part of this work may be reproduced by any process, nor may any other exclusive right be exercised, without the permission of the author. Copyright owners are entitled to take legal action against persons who infringe their copyright. A reproduction of material that is protected by copyright may be a copyright infringement. A court may impose penalties and award damages in relation to offences and infringements relating to copyright material.

Higher penalties may apply, and higher damages may be awarded, for offences and infringements involving the conversion of material into digital or electronic form.

Unless otherwise indicated, the views expressed in this thesis are those of the author and do not necessarily represent the views of the University of Wollongong.

Recommended Citation

Tangboonduangjit, Puangpen, Intensity-modulated radiation therapy dose maps: the matchline effect, PhD thesis, School of Engineering Physics, University of Wollongong, 2006. <http://ro.uow.edu.au/theses/496>

Research Online is the open access institutional repository for the University of Wollongong. For further information contact the UOW Library: research-pubs@uow.edu.au

NOTE

This online version of the thesis may have different page formatting and pagination from the paper copy held in the University of Wollongong Library.

UNIVERSITY OF WOLLONGONG

COPYRIGHT WARNING

You may print or download ONE copy of this document for the purpose of your own research or study. The University does not authorise you to copy, communicate or otherwise make available electronically to any other person any copyright material contained on this site. You are reminded of the following:

Copyright owners are entitled to take legal action against persons who infringe their copyright. A reproduction of material that is protected by copyright may be a copyright infringement. A court may impose penalties and award damages in relation to offences and infringements relating to copyright material. Higher penalties may apply, and higher damages may be awarded, for offences and infringements involving the conversion of material into digital or electronic form.

INTENSITY-MODULATED RADIATION THERAPY

DOSE MAPS: THE MATCHLINE EFFECT

**A thesis submitted in fulfilment of the
requirements for the award of the degree**

DOCTOR OF PHILOSOPHY

From

UNIVERSITY OF WOLLONGONG

By

PUANGPEN TANGBOONDUANGJIT (MSc)

ENGINEERING PHYSICS

2006

Certification

I, Puangpen Tangboonduangjit, declare that this thesis, submitted in fulfillment of the requirements for the award of Doctor of Philosophy, in the Department of Engineering Physics, University of Wollongong, is wholly my own work unless otherwise referenced or acknowledged. The document has not been submitted for qualifications at any other academic institution.

Puangpen Tangboonduangjit

Abstract

In 2002 when this research started the brief of the project was to produce streamlined checks of planar dose maps delivered by IMRT fields to film.

At this time no other centre in Australia had a protocol for checking accuracy of RTP planned RT dose distributions. While many US centers have been checking IMRT distributions, there is still no standard protocol for these checks.

By the end of this project in 2005, 13 IMRT patient treatments had been successfully checked and this centre remains the only centre to have treated IMRT patients in Australia using the pinnacle RTP planning computer platform.

Early film dose maps revealed dose spikes due to MLC matchline effects. These matchlines were due to Varian MLC leaf ends sometimes matching other segment neighbors and were not predicted using pinnacle RTP until version 7.4 available about 2 months prior to the end of this project cycle.

Verifying a radiation treatment planning (RTP) computer's IMRT calculation was the first task for this thesis. Planar dose maps (dose in water perpendicular to the beam [cGy/MU]) were compared with beam dose distributions measured using films (XV and EDR) at various depths. The RTP computer and film measurements agreed within $\pm 3\%$ within the inside field region. In addition, the XV film had a lower linear dose response range than the EDR film, the efficacy of each film type depends on dose

range, the XV being used predominantly for planar dose maps and EDR for combined axial dose maps.

High dose lines (matchline effect) were studied with film measurement. Matchlines were caused by a contribution of extra penumbral dose from MLC transmission due to curved leaf ends. An MLC bank leaf stepping program was used with various minor overlap values (0, 0.06, 0.1, 0.14, 0.2 cm) of MLC position. With confirmation by BEAMnrc Monte Carlo simulations, a dosimetric overlap value due to collective effect of scatter and the rounded leaf end transmission equivalent to 0.09 cm leaf overlap was found for a particular weighting of each segment. Note the physical offset value set to avoid leaf collision is an additional 0.05 cm.

An overlapping co-incident field technique was used to extend field size, this also showed a small jaw-leaf matchline effect at both edges of an overlap region.

An aSi-EPID combined with Varian dosimetry software also showed matchline resolution similar to film. The aSi-EPID, XV film, Pinnacle RTP (version 7.0g and 7.4) and BEAMnrc Monte Carlo were all compared for a 25 segment step and shoot IMRT distribution. IMRT doses in the axial plane were further verified with an IMRT phantom (Scanditronix-Wellhofer) using the EDR and a new low dose radiochromic film (Gafchromic[®] EBT, Lot no. 34267-004). For the irradiated perpendicular calibration setup, dose agreed to within $\pm 5\%$ (1 SD) for EDR and $\pm 4\%$ (1 SD) for Gafchromic[®] EBT film with RTP and an ionization chamber.

The conclusions based on this thesis are the following;

- The matchlines represented a potential overdose to some small volumes within the target dose delivery.
- The matchline patterns produced by moving leaf banks in known sequences helped reveal the physics properties of the rounded leaf end.
- Appropriate physical leaf gaps were found to mask the matchline, however due to differences in segment weights these were not recommended.
- A Monte Carlo model of the Varian 120 MLC was developed using Beam NRC and this model predicted matchline effects.
- EPID dosimetry revealed an a-Si detector array had sufficient spacial resolution to show matchlines.
- Late in cycle Version 7.4 of RTP computer leaf model did predict matchlines of smaller magnitude than experimental results.

Preface

The aims of the thesis

1. In order to verify the TPS system for IMRT technique dose calculation as a pilot study.
2. In order to study the dosimetric leaf end design of MLC which leads to the matchline effect.
3. In order to create benchmark of IMRT dose calculation using Monte Carlo simulation.
4. In order to make a streamline for quality assurance of IMRT technique, EPID and IMRT phantom need to be verified.

Intensity Modulated Radiation Therapy (IMRT)

Intensity-modulated radiation therapy (IMRT) is an advanced 3D conformal radiation therapy technique in which small non uniform dose segments are used to avoid critical organs close to the treatment volume. With the aid of a computer optimization algorithm, a planner specifies dose objectives to the normal tissues and tumour target volumes. Currently the beam energy, field size and beam angle are pre-selected, then the computer iterates until a dose solution is met. The non uniform dose solution is converted to an MLC leaf sequence which would deliver a dose which closely matches this solution. Sometimes a final more accurate calculation proceeds to ensure an accurate final MU which accounts for MLC transmission etc. An overview of

different IMRT delivery including some issue used in this thesis (step & shoot technique, k -means clustering algorithm, CC convolution, Monte Carlo simulation) is described in chapter 1.

IMRT dose verification

Normally a manual calculation is used to check uniform radiation therapy planned treatment fields before the first fraction of dose is going to the patient. However, as mentioned above, IMRT consists of at least several small non uniform dose segments per fields, combined with 7 to 9 fields per fraction to complete an IMRT treatment. As a result a manual calculation for each segment multiplied by each field is time prohibitive. Hence several alternate IMRT dose verification techniques have been developed and there are reviewed in the first section of chapter 2. Because film is the most common for measuring dose in two dimensions, film is the main dosimeter in this thesis. Therefore a few types and the limitations of film dosimeters were reviewed. Moreover the key point of this thesis is studying the dosimetric characteristics of curve leaf end design which leads to the matchline effect, the review of MLC including pros and con of having MLC, the physical leaf end MLC position, and the leaf end transmission was referred in section 2.3. The benchmark of this thesis for IMRT dose verification is using Monte Carlo simulation so various investigations employing Monte Carlo for IMRT modelling were reviewed such as the code types of Monte Carlo simulation, the methods and the code's limitations of modelling curved leaf end MLC. The last section of chapter 2 reviewed the using of electronic portal imaging device (EPID) for IMRT verification. Due to its superior improvements

compared with film dosimeter such as real time imaging and no processing and routine calibration required, it could replace film for IMRT verification in the near future.

Two dimensional dosimeter

When IMRT dose verification first started for patients at Illawara Cancer Care Centre (ICCC) in mid 2002, radiographic film dosimetry was the only method available to compare 2D dose maps with dose predicted from the Pinnacle RTP. Hence film dosimetry is a major part of this thesis. It provides a 2 dimensional high resolution image. It is suitable to verify IMRT fields by visual inspection (qualitative) and dose beam profile (quantitative) measurement. Three types of films were used for this thesis. XV film had the highest sensitivity. The approximate linear dose response range is between 0-100 cGy. EDR film had a linear dose response range between 0-400 cGy. The XV film was mainly used for checking dose per field. The EDR as predominantly used for checking composite field doses. Section 3.2 shows a comparison of results between the XV and EDR film.

Radiochromic film is a more tissue equivalent material ($Z=6.0-6.5$) than radiographic film. There is no processing required. The use of Gafchromic[®] MD-55 is reported in chapter 4 in order to expect the better predicted dose in the region of the MLC penumbral tail due to its linear low energy response characteristics. The results show in section 4.2. Late in 2004, a new Gafchromic[®] EBT film became available, the usage shown in chapter 8. At the same time an Art phantom (Scanditronix-Wellhofer)

became available. This phantom had a better fit and could be clamped tighter than the solid water stacks. So EDR film and Gafchromic[®] EBT were compared for the perpendicular and parallel calibration orientation to the radiation beam. See results in section 8.2. Gafchromic[®] EBT has higher dose sensitivity than MD-55 in order to suit to the clinical radiotherapy dose range (0.01-8 Gy versus 2-100 Gy; www.ispcorp.com).

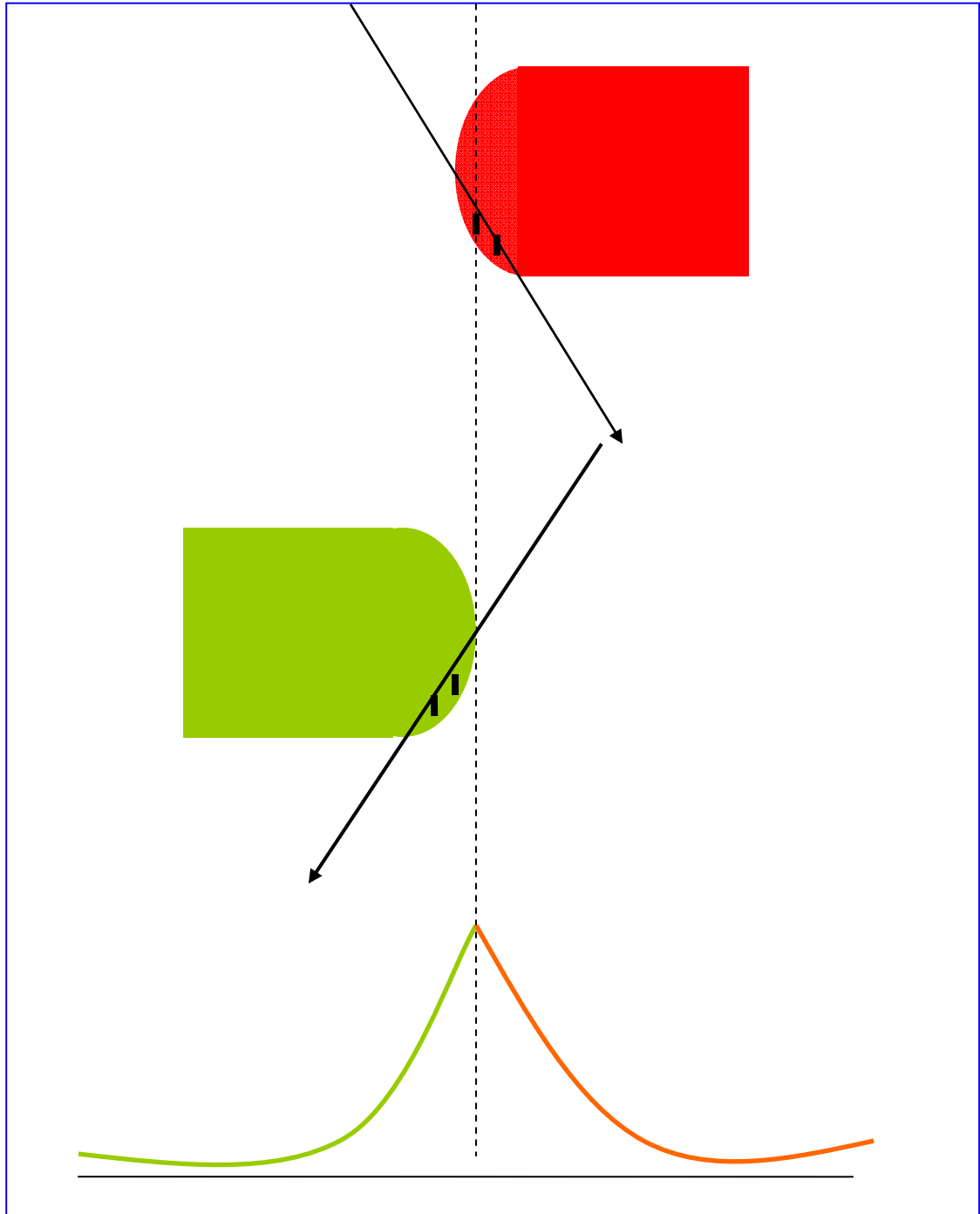
Film analysis was obtained by using a Vidar 12+ scanner for all experiments correspond with Scion analysis program or ImageJ program. The scanner program (Osiris) was calibrated to the OD unit before film scanning therefore the tiff image obtained from the scanner program was automatically related to the OD unit.

In 2005 close to the end of the project time limit, an electronic portal imaging device (EPID) was installed at ICCC with a commercial dose assessment tool. IMRT verification with this device was attractive due to no processing required, online image, and reliability. The aSi-EPID was tested compared with EDR film and BEAMnrc Monte Carlo simulation. The results are discussed in section 7.2.

Matchline effect

During verification of step-and-shoot IMRT fields using the Varian MLC, matchline effects were frequently observed and the detection of these narrow dose lines became a recurring of this thesis. Matchline effects appear due to the curved leaf end design of

this MLC. Extra transmission leads to a combined penumbra (matchline) of extra dose.



The matchline definition: the hot dose line which caused by the combination of the transmission dose (penumbra) through the curved leaf end (tiny vertical lines as shown at the above picture) of MLC pair.

During experiments suitable overlap values of MLC are discussed. An in-house adapted from Hoban P (2002) was used to generate the MLC overlap files. With a confirmation using Monte Carlo simulations, this thesis found an optimal value of MLC overlap which is presented in section 4.2 and 6.2.

In chapter 5, the overlapping co-axial modulated field measurements (film and EPID) and calculation (RTP computer) were compared. Also the effect of matchline appearing between jaw-MLC is discussed. During head and neck IMRT treatment at ICCG, six out of eight head and neck patients treated have had large enough target volumes to require split overlapping co-incident fields (Metcalf *et al* 2004). Because of the limitation of MLC traveling distance up to 14.5 cm, one field was split into 2 subfields with an overlap set at 4 cm.

In chapter 9, the demonstration of the RTP version 7.0g and 7.4 to produce the matchline situation was discussed with a comparison of the clinical IMRT technique with the XV film and MC simulation.

Internationally refereed publications directly related to this work which the author has published during the course of this thesis include the following:

Tangboonduangjit P., Wu I., Butson M., Rosenfeld A., and Metcalfe P., 2003
Intensity modulated radiation therapy: film verification of planar dose maps. *Aust. Phys. Eng. Sci. Med.* **26**: 194-200.

Tangboonduangjit P., Metcalfe P., Butson M., Quach K.Y., and Rosenfeld A., 2004
Matchline dosimetry in step and shoot IMRT fields: a film study. *Phys. Med. Biol.* **49**: N287-N292.

Associated papers in this area which the candidate has had significant input into include:

Metcalfe P., Chapman A., Arnold A., Arnold B., Tangboonduangjit P., Capp A., and Fox C., 2004 Intensity-modulated radiation therapy: Not a dry eye in the house. *Australasian Radiology* **48**: 35-44.

Metcalfe P., Tangboonduangjit P., and White P., 2004 Intensity-modulated radiation therapy: overlapping co-axial modulated fields. *Phys. Med. Biol.* **49**: 3629-3637.

Parts of this work have also been presented by the author at the following conferences:

Tangboonduangjit P., Metcalfe P., Butson M., Quach K.Y., and Rosenfeld A.
Intensity-modulated radiation therapy (IMRT) dose verification: measuring the match line effect. **World congress on Medical Physics and Biomedical Engineering conference, Sydney Australia, 24-29 August 2003.**

Tangboonduangjit P., Metcalfe P., Butson M., Quach K.Y., and Rosenfeld A.
Intensity-modulated radiation therapy (IMRT) dose verification: measuring the match line effect. **Experimental Radiation Oncology, St.George Hospital, Sydney Australia, Dec, 2003.**

Tangboonduangjit P., Metcalfe P., Takacs G., and Rosenfeld A. Monte Carlo simulation of a linear accelerator for a 6 MV photon beam. **Experimental Radiation Oncology, University of Newcastle, Collaghan, NSW, 6 Dec, 2004.**

Acknowledgements

I am very grateful to my supervisor Prof. Peter Metcalfe for his consultation, extensive help, and assiduous meeting discussion. Thanks also to Prof. Anatoly Rosenfeld for providing me with valuable discussions about the project.

Thanks to Assoc. Prof. Martin Butson for film dosimetry consultation, Dr. Martin Carolan for help with EPID measurements, Kim Quach with Linac based experimental help and Dr. Mathew Williams with the RTP V7.4 discussion. I also thank all staff of ICCC for their cooperation and friendship.

I would like to thank Dr. George Takacs for Monte Carlo simulation consultation and also Mr. Fredrik Hilding for his script which helped with Monte Carlo simulation. And also Dr. Peter Hoban for supplying the MLC leaf overlap program.

Thanks are also given for my class mate and all staff of Centre for Medical Radiation Physics (CMRP) for their encouragement and inspiration.

I wish to acknowledge my financial support by Thai government and Ramathibodi Hospital.

Finally, my greatest thanks is to my family: my parents Chanchai and Orapin Tangboonduangjit, and my two younger brothers Aroon and Aram Tangboonduangjit for their love and support.

Table of Contents

Abstract	i
Preface	v
Acknowledgements	xiii
Table of Contents.....	xv
List of Tables.....	xxi
List of Figures	xxiii
Chapter 1: Introduction	1
1.1. Introduction.....	1
1.2. The planning processes of IMRT.....	3
1.2.1. Optimization algorithm	3
1.2.2. Leaf sequencing algorithms.....	7
1.2.3. Dose calculation algorithms	13
1.3. Techniques to deliver Intensity modulated beams.....	16
1.3.1. Conventional MLC IMRT.....	16
1.3.2. Scanned beam IMRT	17
1.3.3. Tomotherapy IMRT	18
1.3.4. Physical modulator IMRT.....	18
Chapter 2: Literature Review	21
2.1. Verification of IMRT	21
2.2. Film dosimeters	23
2.3. Multileaf Collimator (MLC)	25

2.4. Monte Carlo with MLC simulation	30
2.5. Electronic Portal Imaging Devices (EPID)	34
Chapter 3: Intensity modulated radiation therapy (IMRT): film verification of planar dose maps.....	39
3.1. Materials and methods.....	40
3.1.1. The Radiotherapy Treatment Planning Software.....	40
3.1.2. The planar dose map tool	43
3.1.4. Benchmark of film dosimeter for conventional field techniques	46
3.1.5. Benchmark of film dosimeter for IMRT field technique with other detectors	46
3.1.6. Comparison of film measurement with the RTP computer for a conventional field technique and an IMRT field.....	47
3.2. Results and discussion.....	47
3.2.1. The planar dose map tool	47
3.2.2. Film calibration.....	48
3.2.3. Benchmark of film dosimeter for conventional field technique.....	49
3.2.4. Benchmark of film dosimeter for IMRT field technique.....	50
3.2.5. Comparison of film measurement with the RTP computer for a conventional and an IMRT field.....	52
3.3. Summary and conclusion.....	57
Chapter 4: Intensity-modulated radiation therapy (IMRT): measuring the matchline effect	59
4.1. Materials and methods.....	59
4.2. Results and discussion.....	64
4.3. Summary and Conclusion	70
Chapter 5: Intensity-modulated radiation therapy (IMRT): overlapping co-axial modulated fields	73

5.1. Materials and methods	74
5.2. Results and discussion	75
5.3. Summary and Conclusion	82
Chapter 6: Monte Carlo simulations	85
6.1. Materials and methods	85
6.1.1. Validate Monte Carlo code for 10x10 cm ² field	85
6.1.2. Validate the geometry of multileaf collimator	87
6.1.3. Apply code to the clinical IMRT matchline field.....	91
6.2. Results and discussion	95
6.2.1. Validate Monte Carlo code for 10x10 cm ² field.....	95
6.2.2. Validate the geometry of multileaf collimator	103
6.3. Summary and Conclusion	117
Chapter 7: Intensity-modulated radiation therapy (IMRT): EPID measurement	119
7.1. Materials and methods	119
7.1.1. EPID calibration	119
7.1.2. EPID measurements	120
7.1.3. Film measurement.....	121
7.2. Results and discussion	121
7.3. Summary and Conclusion	125
Chapter 8: Intensity modulated radiation therapy (IMRT): Parallel film verification with an I'mRT phantom.	127
8.1. Materials and Methods.....	128
8.1.1. Single field and four field technique verification	128
8.1.2. IMRT field technique verification	130

8.1.3. Film analysis	133
8.1.4. Ionization chamber measurement	134
8.2. Results and Discussion	134
8.3. Summary and Conclusion	143
Chapter 9: The RTP version 7.0g & 7.4: matchline comparison	147
Chapter 10: Conclusion	157
References	161
Appendix A: The comparison of jaw and MLC's dose profiles.	175
Appendix B: The mlctable.txt.....	179
Appendix C: The .mlc file	181
Appendix D: Monte Carlo input and output files.....	183
D.1. Input and output files for BEAMnrc code simulated from target to mirror.	183
D.1.1. Input file: LA6_1.egsinp	183
D.1.2. Output file: LA6_1.egslst.....	188
D.2. Input and output files for BEAMnrc between secondary collimator jaw to the air slab.....	204
D.2.1. Input file: LA7_7imrt5-f07.egsinp	204
D.2.2. Output file: LA7_7imrt5-f07.egslst.....	206
D.3. Input and output files for DOSXYZnrc	215
D.3.1. Input file: DoseLA7_7imrt5-f07.egsinp	215
D.3.2. Output file: DoseLA7_7imrt5-f07.egslst.....	216
Appendix E: EGSnrc with BEAMnrc and DOSXYZnrc's parameters	225

Appendix F: Hoban’s MLC file program227

Appendix G: The interpretation of MLC positions229

**Appendix H: The reference marker distances of the Art phantom
.....231**

List of Tables

Table 2- 1 The verification of IMRT from various investigated groups.....	22
Table 3- 1. Central axis point dose (Gy) data of IC4, EDR film, and RTP computer of a conventional field at 100 cm SSD at 1.5, 7.5, and 15 cm depth.	50
Table 3- 2. Central axis point dose (Gy) data of IC4, EDR film, and RTP computer of an IMRT field at 100 cm SSD at 1.5, 7.5, and 15 cm depth.	55
Table 4- 1. Summary of relative dose ratio between peak (P) and valley (V) dose and the average relative dose as well as standard deviation (Stdev) of XV, EDR radiographic films and MD-55-2 radiochromic film at various overlap values: (6 MV, field size 12×12 cm ² , depth 1.5 cm for SSD 100 cm).....	67
Table 4- 2. Relative dose measurement of XO-mat V, EDR2 radiographic films, MD-55-2 normalized to Ionization chamber at off axis point from central beam 1 cm at 0 cm overlap values.	70
Table 6- 1. The segment numbers and the position of leaves. These MLC positions were observed in the IMRT.MLC file provided in the Appendix C.	93
Table 6- 2. The summary of parameters for the Monte Carlo simulation of 3 experiments. The computer used for running MC is Pentium-Celeron 1.5 MHz.	95
Table 6- 3. The standard deviations for the matchline 2 and 3-4 with the overlap value 0, 0.08, 0.1, 0.12, 0.14 cm for a 6 MV beam at depth 1.5 cm with 100 cm SSD.	116
Table 8- 1. The MU/fraction for each IMRT-beam using 6 MV beams.	131
Table A- 1. Beam profile parameters measured from Figure A-2 using equation (1) and (2), for a 6 MV beam, field size 2×12 cm ² at depth dmax, SSD 100 cm. ..	177

Table A- 2. The values of α_1 and α_2 of Jaw and MLC derived from equation (1) and (2) respectively (6 MV beam, field size 2×12 cm² at depth dmax, SSD 100 cm).
..... 178

Table B- 1. MLCTABLE.TXT for the Varian Millennium MLC 180

Table C- 1. An example of .mlc file of the 3 segmented clinical IMRT technique generated from Pinnacle at the number of Fields = 12, the number of leaves = 120, and tolerance = 0.5 181

Table F- 1. The position of MLC in cm of 2 different setup of matchline offset. 227

List of Figures

Figure 1- 1. The example diagram shows the delivery of the intensity pattern by the areal step-and-shoot technique.	12
Figure 3- 1. Illustration of the steps for IMRT planning on Philips Pinnacle RTP computer.	41
Figure 3- 2. Planar dose and a film inverted optical density map. (The lighter area of density represents higher radiation absorbed dose). (Photon beam 6 MV at 15 cm depth at 100 cm SSD).....	48
Figure 3- 3. The comparison of dose response between EDR and XV films. (Field is 6 MV at 10×10 cm ² , 15 cm depth at 100 cm SSD).	49
Figure 3- 4. Comparison of dose beam profiles between the Sun Nuclear Profiler, EDR and XV films for IMRT field technique using a 6 MV beam at 15 cm depth at 100 cm SSD.	51
Figure 3- 5. Dose beam profiles compared between RTP computer and EDR film for a conventional field technique at (a) d _{max} , (b) d = 7.5 cm, and (c) d = 15 cm....	53
Figure 3- 6. IMRT dose profiles along the crossplane (a) and inplane (b) compared between EDR film and RTP computer at three different depths for 6 MV with 100 cm SSD.	55
Figure 4- 1. The example of 2 step MLC movement of leaf pair 1B-1A and leaf pair 2B-2A; (a) shows the gap width value 2 cm and (b) illustrates the gap width value 1.86 cm.....	61
Figure 4- 2. XV-film measurement of matchline effect (6 MV, field size 12×12 cm ² , depth 1.5 cm for SSD 100 cm): (a) overlap 0 cm, (b) overlap 0.06 cm, (c) overlap 0.1 cm, (d) overlap 0.14 cm, (e) overlap 0.2 cm.	65
Figure 4- 3. (a) The %relative dose beam profile of XV film illustrated 5 matchlines at overlap 0 cm. (b) The average of the %relative dose matchline beam profiles of XV, EDR radiographic films, MD-55-2 films at overlap 0 cm. (6 MV, field size 12×12 cm ² , depth 1.5 cm for SSD 100 cm).....	66

Figure 4- 4. Average of the %relative dose matchline beam profiles of Kodak XV film at the overlap 0, 0.06, 0.1, 0.14, and 0.2 cm. (6 MV, field size 12×12 cm ² , depth 1.5 cm for SSD 100 cm).....	68
Figure 4- 5. Standard deviation along average relative dose (%) of a beam profile of XV, EDR radiographic films, MD-55-2 films for each overlap value of leaf: (6 MV, field size 12×12 cm ² , depth 1.5 cm for SSD 100 cm).....	68
Figure 5- 1. (a) and (b) show two subfields of planar dose maps from the Pinnacle RTPS a 6 MV beam at 98.5cm SSD and depth at d _{max} . (c) shows dose beam profile comparison among Figure 5- 1(a), (b), and the combined dose profiles between Figure 5- 1(a) and (b).....	77
Figure 5- 2. (a), (b), and (c) XV-Film planar optical density maps of the first and second subfields and the combined of 2 subfields respectively (a 6 MV beam at 98.5cm SSD and depth at d _{max}). (d) shows the dose beam profiles which display how the two dose peaks occur.....	80
Figure 5- 3. The aSi-EPID image obtained for a 6 MV beam at depth 1.5 cm with 98.5 cm SSD with courtesy by Paul White, Nepean Cancer Care.	80
Figure 5- 4. Comparison of dose profile graphs of RTPS for a 6 MV at depth 1.5 cm with 98.5 cm SSD.....	81
Figure 6- 1. (a) X Cross-sectional view of a VARMLC component module by Monte Carlo simulation comparing to (b).1 X Cross-sectional and (b).2 the lateral view of the Varian 120 millennium MLC leaf.....	89
Figure 6- 2. (a) BEAMnrc simulation showing the component modules of Varian linac 2100C of a photon mode. (b) BEAMnrcMP simulation (the latest version which can be run on the windows operating system) showing the same Varian linac 2100C of a photon mode.	97
Figure 6- 3. Comparison of 6 MV photon beam profiles of field size 10×10 cm at SSD 100 cm of (a) depth 5 cm and (b) depth 10 cm. The diamond symbol indicates simulation using MC simulation.	98

Figure 6- 4. Comparison of a 6 MV photon beam depth dose, field size $10\times 10\text{ cm}^2$ at 100 cm SSD (a) depth from 0 to 20 cm. (b) Depth from 0 to 1 cm. The square symbol represents the MC simulation. 100

Figure 6- 5. (a) Comparison of %relative dose beam profile of a 6 MV beam (FWHM 0.1 cm) with field size $10\times 10\text{ cm}^2$ at depth 5 cm of 100 cm SSD. (b) shows the comparison of the penumbra region on one side when the scale is expanded and narrowed. 101

Figure 6- 6. Comparison of %relative dose beam profile of a 6 MV beam (FWHM 0.2 cm) with field size $10\times 10\text{ cm}^2$ at depth 5 cm of 100 cm SSD. (b) shows the comparison of the penumbra region on one side when the scale is expanded and narrowed. 102

Figure 6- 7. A photon spectral distribution of 6 MeV incident electron energy with 2-D particle distribution FWHM 0.1 cm at 100 cm SSD for $10\times 10\text{ cm}^2$ field size. 103

Figure 6- 8. Comparison of closed MLC leaf end dose distribution for a 6 MV beam at depth 1.5 cm and 100 cm SSD. The triangular symbol represents the MC simulation (collimator jaws set at $10\times 10\text{ cm}^2$). 105

Figure 6- 9. Comparison of matchline beam profiles parallel to the MLC drive direction for a 6 MV beam at depth 1.5 cm of 100 cm SSD. (a) shows the whole MLC steps of matchline beam profile, (b) represents the average matchline beam profiles of XV film and MC simulation. 107

Figure 6- 10. The comparison of the average matchline beam profile compared between the MC and the re-do experiment of XV film measurement with no leaf gap and resolution 0.2 cm/pixel shown as a square symbol, at depth 1.5 cm, SSD 100 cm and 6 MV beam of Varian 2100C. 109

Figure 6- 11. The comparison of XV film measurement and MC simulation of the average matchline beam profile with re-set of XV film resolution pixel to 0.2 cm shown as a square symbol at depth 1.5 cm, SSD 100 cm and 6 MV beam of Varian 2100C. 110

Figure 6- 12. XV-film measurement of the first 3 segment of the 25 segment IMRT field technique for a 6 MV beam at depth 1.5 cm with SSD 100 cm. 111

Figure 6- 13. Comparison of dose beam profiles between XV film and MC simulation for the MLC 3 segment-IMRT field with a 6 MV beam at depth 1.5 cm of 100 cm SSD.	112
Figure 6- 14. The XV-film image of the completed 25 segments of IMRT technique for a 6 MV beam at 100 cm SSD and depth 1.5 cm.	113
Figure 6- 15. Comparison of dose beam profile parallel to the MLC moving between the XV film measurement and the Monte Carlo simulation for a 6 MV beam at depth 1.5 cm with 100 cm SSD.	114
Figure 6- 16. Comparison of dose beam profile parallel along the MLC moving of the completed segment-IMRT field with various overlapped values for a 6 MV beam at depth 1.5 cm of 100 cm SSD.	115
Figure 6- 17. The enlarged graph from Figure 6- 16 shows the range of the standard deviation calculation for each matchline.	116
Figure 7- 1. The standard field size $10 \times 10 \text{ cm}^2$ of an EPID image for a 6 MV beam at 105 cm SDD [Source detector distance]: (a) planar dose map and (b) dose beam profile across centre of dose map.	122
Figure 7- 2. (a) shows the IMRT-image from EPID data of a 6 MV beam at 105 cm SDD. (b) shows a dose beam profile in the calibration unit (CU) data.	124
Figure 7- 3. Comparison of the dose beam profile of the completed-IMRT field at depth 1.5 cm of 100 cm SSD for a 6 MV beam.	125
Figure 8- 1. The humanoid I'mRT phantom (local name "Art phantom") in this study, (a) parallel radiographic film setup for 4 axial planes, (b) and (c) show the superior and inferior view of the phantom respectively.	133
Figure 8- 2. The standard film calibration curves using a 6 MV beam with SAD technique for field size $15 \times 15 \text{ cm}^2$, comparison between parallel (pll) and perpendicular (pdc) setup of (a) EDR film at depth 10 cm and (b) Gafchromic EBT at depth 9 cm.	136
Figure 8- 3. The film image (jpeg file) using a digital camera of IMRT field technique at isocenter (slice 0 cm) in the parallel setup of a 6 MV beam by (a) the EDR film and (b) the Gafchromic film.	139

Figure 8- 4. The histogram point dose using a 6 MV beam at the location of the isocenter point (0 cm) to the superior direction 2 and 4 cm compared between EDR for pdc (perpendicular) and pll (parallel) calibration with RTP for (a) 1 field, (b) 4 field techniques for field size 15×15 cm², and (c) IMRT technique with additional comparison points with IC (CC13). 141

Figure 8- 5. The histogram point dose using a 6 MV beam at the location of the isocenter point (0 cm) to the superior direction 2 and 4 cm compared between Gafchromic EBT film for perpendicular (pdc) and parallel (pll) calibration with RTP for (a) 1 field, (b) 4 field techniques for field size 15×15 cm², and (c) IMRT technique with additional comparison points with IC (CC13)...... 143

Figure 9- 1. The two dimensional images of IMRT technique using a 6 MV beam at depth 1.5 cm with 100 cm SSD. (a)-1 shows planar dose map image of the RTP with resolution 0.5 cm/pixel, (a)-2 shows the %relative isodose of the RTP, (b) shows XV-film image resolution 60 DPI (0.0423 cm/pixel), (c) aSi-EPID image with resolution 0.058 cm/pixel, and (d) MC simulation image for 0.2 cm/pixel. 150

Figure 9- 2. (a) Comparison of dose beam profiles of the RTP version 7.0g, XV film, aSi-EPID, and MC simulation for the same IMRT technique as in Figure 9- 1 at the position 0.75 cm superior of the beam center. (b) is the enlarged scale of (a). 150

Figure 9- 3. The matchline dose beam profiles generated with the RTP V7.4 (leaf radius 18 cm and transmission 1.8%) for different calculation dose grid size as following: 0.15, 0.2, and 0.4 cm with planar dose map pixel size 0.1, 0.2, and 0.2 cm respectively at depth 1.5 cm, 100 cm SSD with a 6 MV photon beam. 151

Figure 9- 4. Comparison of the RTP version 7.0g dose beam profile of 3 segmented IMRT technique at depth 1.5 cm of a 6 MV photon beam with the XV film and MC simulation. 152

Figure 9- 5. Comparison of the RTP version 7.0g and 7.4 (dose grid size 0.2 cm and planar dose map pixel size 0.1 cm) dose beam profile of 3 segmented IMRT technique at depth 1.5 cm of a 6 MV photon beam with the XV film and MC simulation. 153

Figure 9- 6. The image of the planar dose map in grey scale of the RTP Pinnacle version 7.4 of the 25 segmented IMRT technique at depth d_{max} of a 6 MV photon beam. 154

Figure 9- 7. (a) shows the comparison of the RTP version up to 7.0g and 7.4 (dose grid size 0.2 cm and pixel size 0.1 cm) dose beam profile of 25 segmented IMRT technique at depth 1.5 cm of a 6 MV photon beam with the XV film and MC simulation. (b) is enlarged scale of (a). 155

Figure 9- 8. The comparison of XV film measurement, MC simulation and the RTP version 7.4 (leaf radius 12 cm and leaf transmission 1.5%) of the average matchline beam profile with no physical leaf gap between leaf pair condition at depth 1.5 cm, SSD 100 cm and 6 MV beam of Varian 2100C. 155

Figure A- 1. A schematic of the penumbral dose profile with the parameters defined on the schematic. 176

Figure A- 2. Experimental beam profile data comparison between Secondary collimator jaw and MLC using EDR film. (6 MV beams, field size $2 \times 12 \text{ cm}^2$ at depth d_{max} , SSD 100 cm). 177

Figure B- 1. Diagram showing the relation between the light-field edge and the leaf-tip distance (Boyer and Li 1997). 179

Figure G- 1. (a) The direction sign of MLC moving of 120 millennium Varian MLC. (b) The direction sign of MLC moving of the Monte Carlo simulation by VARMLC component module. 230

Figure G- 2. The example of the illustration of MLC moving. MLC A is at the position 0 cm and MLC B moves away from the central axis or moves to the left from the central axis 2 cm. 230

Figure H- 1. The reference marker distances of the Art phantom. 231